

Active feedback cooling of massive electromechanical quartz resonators

Junghoon Jahng,^{*} Manhee Lee, Corey Stambaugh, Wan Bak, and Wonho Jhe[†]

Center for Nano-Liquid, Department of Physics and Astronomy, Seoul National University, Seoul 151-747, Korea

(Received 7 April 2011; published 11 August 2011)

We present a general active feedback cooling scheme for massive electromechanical quartz resonators. We cool down two kinds of macrosized quartz tuning forks and find several characteristic constants for this massive quartz-resonator feedback cooling, in good agreement with theoretical calculations. When combined with conventional cryogenic techniques and low-noise devices, one may reach the quantum sensitivity for macroscopic sensors. This may be useful for high sensitivity measurements and for quantum information studies.

DOI: [10.1103/PhysRevA.84.022318](https://doi.org/10.1103/PhysRevA.84.022318)

PACS number(s): 03.67.-a, 07.10.Cm, 85.85.+j, 37.10.Mn

I. INTRODUCTION

The prospect of cooling a nanomechanical resonator [1], for which the quantum limit can be achieved when the vibrational energy $\hbar\omega_0$ of the resonator becomes smaller than the thermal energy $k_B T_0$, has led to extensive studies [2–13]. When the nanomechanical systems are cooled close to their ground states by conventional cryogenic techniques, they are expected to be useful tools for studying quantum effects such as backaction reaction [2,5,12], coherent states, and superposition [3,4] of macroscopic mechanical systems. In particular, when coupled to other quantum systems, quantum information and computation studies are possible [14–16].

However, since conventional cryogenic techniques only allow cooling to the milli-Kelvin region, it is difficult to realize the ground state of a resonator. For example, a resonator in the frequency range of a few mega-Hertz has to be cooled down to a few hundred micro-Kelvin as given by $\hbar\omega_0/k_B$. Therefore, in combination with conventional cryogenic techniques, researchers have investigated the cooling of the fundamental mode of a mechanical oscillator by using feedback methods. Many oscillators such as cavity resonator and superconducting single-electron transistor have been investigated by using either optomechanical [2–5,7–10] or electromechanical [11–13] cooling techniques, and by implementing either active feedback [7–11] or passive backaction effects [2–5,12,13].

According to these studies, the best desirable oscillator would possess high angular resonance frequency ω_0 , high mechanical quality factor Q_0 , low measurement noise $\sqrt{S_{x_n}}$, and low spring constant k [7–11]. Given the stated requirements of the above factors, we make a theoretical and experimental study of the electromechanical quartz resonator which offers a wide range of attainable frequencies (10^3 – 10^9 Hz), high Q_0 (10^4 – 10^6), and extremely low measurement noise properties [17]. In particular, a quartz resonator has self-excitation and self-detection properties so that additional excitation and detection components are not needed. This approach may be advantageous for the feedback cooling mechanism: (i) exclusion of the supplementary instruments which can simplify fabrication and allow compact integration into a cryogenic system and (ii) elimination of the optical measurement noise

and the associated laser-absorption heating effect found in optomechanical systems [9].

In this article, we present comprehensive theoretical analysis and experimental realization of an active feedback cooling mechanism for massive quartz resonators by implementing the Q -control scheme [18] which is a technique to control the damping of the resonator. Since we derive the feedback cooling theory of a general equivalent circuit of a quartz resonator, this cooling mechanism can be conventionally applied to any nanomechanical and macromechanical quartz resonators. Our cooling result should extend from nanomechanical to macrosized quartz resonators modeled by Fig. 1(c). We conduct the experiment with quartz tuning forks which are widely used as a probe in scanning probe microscopy [19–25]. We obtain several deterministic parameters for massive quartz-resonator cooling, in good agreement with theoretical calculations. Finally, we discuss the way to approach the quantum limit in macroscale, and suggest possible measurements using this system.

II. THEORY

The quartz tuning fork (QTF) is a self-oscillating and self-sensing resonator. Its self-exciting and self-detecting properties can be represented by an electrical equivalent circuit model composed of a series LRC circuit, which describes the mechanical response of the resonator, in parallel with a structure-dependent stray capacitance C_0 resulting in the nonmotional response [26,27]. The measurement noise current is added to the output current of the QTF and converted to a voltage by a current-to-voltage amplifier. The output voltage is then bifurcated into two parts. One part goes into a spectrum analyzer and the other part is used as a feedback signal to the QTF after passing through a phase shifter and proper gain control. The equation of motion for the active feedback cooling of QTF is

$$\begin{aligned} L\ddot{I}_m + R\dot{I}_m + \frac{I_m}{C} &= \dot{V}_{\text{th}} - GR_0(I_m + I_{C_0} + I_{x_n}), \\ I_{C_0} &= C_0[\dot{V}_{\text{th}} - GR_0(I_m + I_{C_0} + I_{x_n})], \\ V_{\text{out}} &= V_m + V_{C_0} + V_{x_n} = R_0(I_m + I_{C_0} + I_{x_n}). \end{aligned} \quad (1)$$

Here L , R , C are the intrinsic components of the QTF's harmonic motion, G is a complex gain which takes into account the effects of the phase shifter, and R_0 is the resistance of the I/V converter. In addition, I_m is the current of the mechanical motion, I_{C_0} is the current induced by C_0 , V_{th} is the

^{*}kingijh1@snu.ac.kr

[†]whjhe@snu.ac.kr

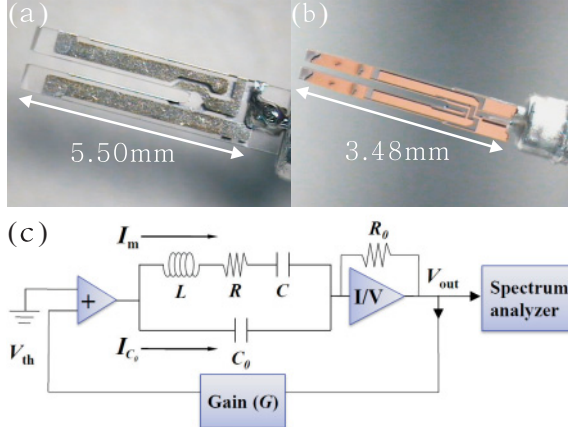


FIG. 1. (Color online) Commercial quartz tuning fork (QTF). (a) The large and (b) the small QTF. (c) General active feedback cooling schematic of a self-exciting and self-detecting quartz resonator by implementing Q -control scheme.

electrically scaled random thermal noise force, $I_{x_n} = V_{x_n}/R_0$ is the measurement current noise on the displacement signal, and V_{out} is the voltage measured at the spectrum analyzer.

According to the equipartition theorem, the effective temperature of the tuning fork can be defined as $T_{eff} = k\langle x^2(t) \rangle / k_B$ where $\langle x^2(t) \rangle = \frac{1}{2\pi} \int S_x(w) dw$; w is the angular frequency and k_B is the Boltzmann constant. We can obtain the actual mechanical displacement $x(t)$ from $I_m(t)$ by multiplying the voltage to displacement calibration factor γ by the relation $x(t) = \gamma R_0 I_m(t)$. Given Eq. (1) and considering frequency components of the random excitations $\tilde{V}_{th}(w)e^{iwt}$ and $\tilde{I}_{x_n}(w)e^{iwt}$, the motion of the oscillator can be given as the familiar expression for a harmonic oscillator;

$$\tilde{I}_m(w) = \frac{i\omega C \tilde{V}_{th}(w) - i\bar{w} \frac{|g|}{Q} \tilde{I}_{x_n}(w)}{1 - \bar{w}_{eff}^2 + i\bar{w}_{eff}/Q}, \quad (2)$$

where $w_0 = 1/\sqrt{LC}$, $\bar{w} = w/w_0$, $\bar{w}_{eff} = w/w_{eff}$, $g = GR_0Cw_0Q = |g|e^{i\theta}$, and $Q = Lw_0/R$. The effective angular resonance frequency w_{eff} and effective quality factor Q_{eff} in Eq. (2) are defined as

$$w_{eff} = \frac{w_0}{\sqrt{1 + \frac{|g|}{Q_0} \sec \alpha \sin(\theta + \alpha)}}, \quad (3)$$

$$Q_{eff} = Q_0 \frac{\sqrt{1 + \frac{|g|}{Q_0} \sec \alpha \sin(\theta + \alpha)}}{1 + |g| \sec \alpha \cos(\theta + \alpha)}, \quad (4)$$

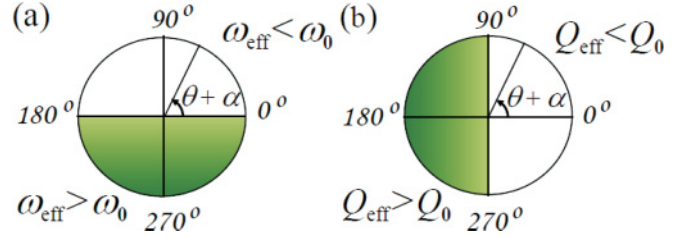


FIG. 2. (Color online) Diagram of the effective resonance frequency and effective quality factor. The w_{eff} and Q_{eff} are bigger (smaller) than their normal value in the shaded (white) region.

where $\tan \alpha = \frac{\bar{C}_0}{Q}$, $\bar{C}_0 = C_0/C$, and α is the initial phase shift which comes from the stray capacitance of the QTF [18]. In order to clearly understand the behavior of effective angular resonance frequency and effective quality factor, it is convenient to draw diagrams of them with phase shift $\theta + \alpha$ and gain. Figure 2 definitely shows that to avoid the resonance shift and to approach the minimum quality factor, θ has to be $-\alpha$. In our case, $\alpha = 0.5^\circ$ for the large QTF and $\alpha = 0.4^\circ$ for the small QTF.

Since the random excitations $\tilde{V}_{th}(w)$ and $\tilde{I}_{x_n}(w)$ are uncorrelated, the spectral density $S_x(w)$ of the oscillator's displacement x is

$$S_x(w) = \frac{S_{th} + \frac{|g|^2}{Q^2} S_{x_n}}{(1 - \bar{w}_{eff}^2)^2 + (\frac{\bar{w}_{eff}}{Q_{eff}})^2} \bar{w}^2, \quad (5)$$

where $S_{th} = \frac{2\pi}{T} (\frac{R_0}{Q_0 R})^2 |\tilde{V}_{th}(w)|^2 \gamma^2$ is the white spectral density of thermal noise force V_{th} , which depends on the QTF dissipation and is given by $S_{th} = 4k_B T / k w_0 Q C^2$, and $S_{x_n} = \frac{2\pi}{T} R_0^2 |\tilde{I}_{x_n}(w)|^2 \gamma^2$ is the spectral density of measurement noise. Its measured spectral density S_{x+x_n} , which contains both S_x and S_{x_n} , is given by

$$S_{x+x_n}(w) = \frac{[1 + \bar{C}_0(1 - \bar{w}^2)^2]^2 + (\frac{\bar{C}_0 \bar{w}}{Q_0})^2}{(1 - \bar{w}_{eff}^2)^2 + (\frac{\bar{w}_{eff}}{Q_{eff}})^2} \bar{w}^2 S_{th} + \frac{(1 - \bar{w}^2)^2 + (\frac{\bar{w}}{Q_0})^2}{(1 - \bar{w}_{eff}^2)^2 + (\frac{\bar{w}_{eff}}{Q_{eff}})^2} S_{x_n}, \quad (6)$$

where $\bar{w} = w/w_0$.

By integrating Eq. (5) and assuming that S_{th} and S_{x_n} are independent of w , the effective temperature is

$$T_{eff}(w_{eff}, Q_{eff}) = \left(\frac{w_{eff}}{w_0}\right)^3 \frac{Q_{eff}}{Q_0} T_0 + \frac{k}{4k_B} \frac{Q_{eff}^2 Q_0^2 (w_0^2 - w_{eff}^2)^2 + w_{eff}^2 (w_0 Q_0 - w_{eff} Q_{eff})^2}{w_{eff} Q_{eff} w_0^2 (Q_0^2 + \bar{C}_0^2)} S_{x_n}, \quad (7)$$

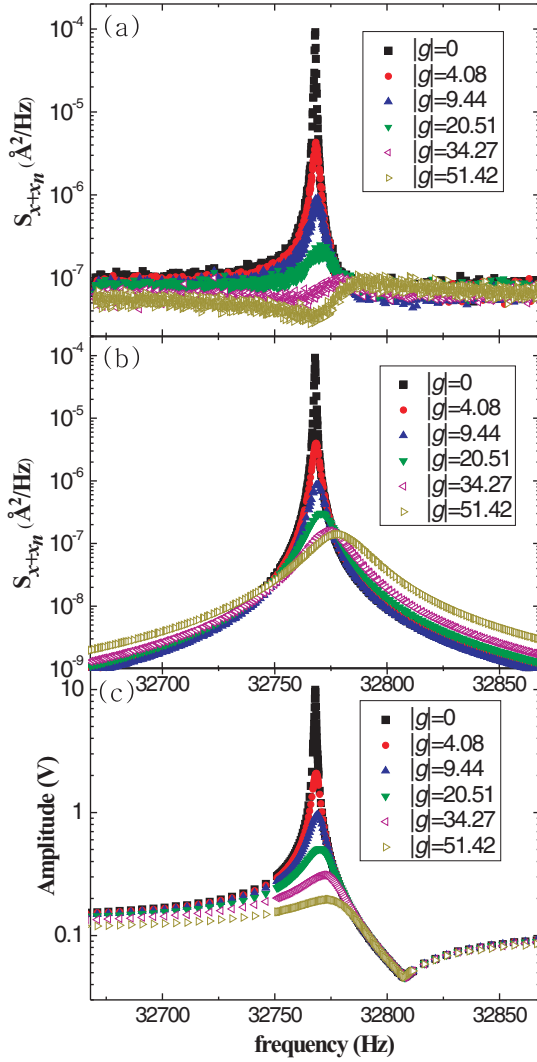


FIG. 3. (Color online) (a) Measured spectra S_{x+x_n} with each gain and their fits with Eq. (6) for the large QTF. (b) The actual displacement spectral density S_x for a large QTF is obtained with Eq. (5) by extracting parameters from S_{x+x_n} . (c) Resonance curves of the electrically driven large QTF for each gain. The solid lines are fits to the data using Eq. (9).

where T_0 is the bath temperature. Since w_{eff} and Q_{eff} are a function of $|g|$, the minimum temperature is calculated by differentiating Eq. (7) with respect to $|g|$ and setting $\theta = -\alpha$:

$$T_{\text{eff,min}} \simeq \sqrt{\frac{Q_0^2}{Q_0^2 + \bar{C}_0^2} \frac{k w_0 T_0}{k_B Q_0} S_{x_n}}. \quad (8)$$

This is very similar to Eq. (6) of Ref. [9]. The only difference is \bar{C}_0 , which is an intrinsic property of QTF resulting from its material and structural properties. Even though \bar{C}_0 gives the unwanted artifact in Figs. 3 and 4, it can be exactly pointed out and moreover it helps to further decrease down $T_{\text{eff,min}}$ [28].

III. EXPERIMENTAL DETAILS

Our experimental setup is a homemade QTF based atomic force microscope operated in vacuum ($P < 1 \times 10^{-5}$ Torr). We used two kinds of commercial QTF. One has a length

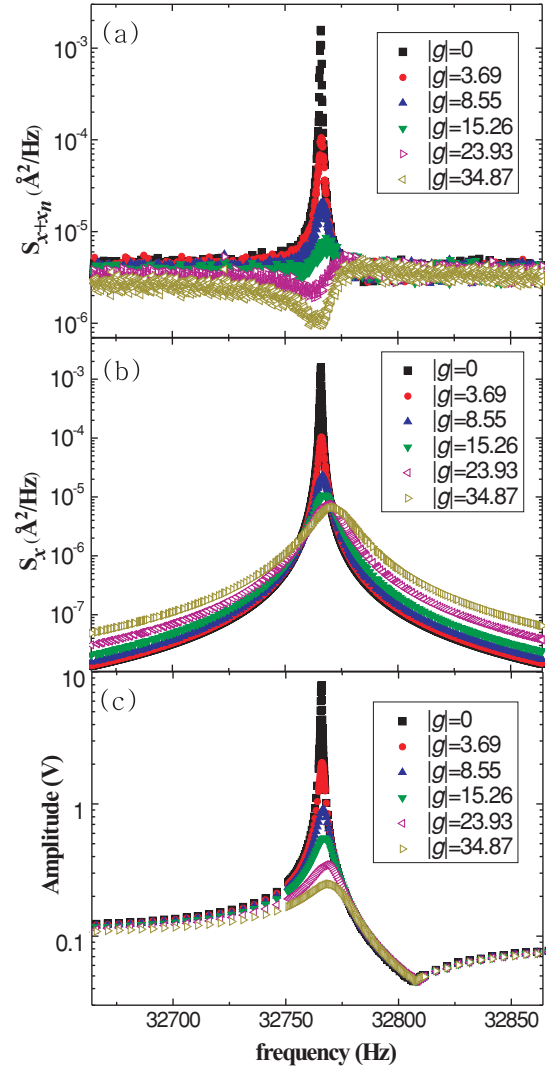


FIG. 4. (Color online) (a) Measured spectra S_{x+x_n} with each gain and their fits with Eq. (6) for the small QTF. (b) The actual displacement spectral density S_x for a small QTF is obtained with Eq. (5) by extracting parameters from S_{x+x_n} . (c) Resonance curves of the electrically driven small QTF for each gain. The solid lines are fits to the data using Eq. (9).

of 5.50 mm, an effective mass of 1.31 mg, and a spring constant k of 55 679 N m $^{-1}$. The other has a smaller length of 3.48 mm, an effective mass of 0.08 mg, and k of 3342 N m $^{-1}$. The natural resonance frequency $\omega_0/2\pi$ and the quality factor Q_0 are $\omega_0/2\pi = 32\,768$ Hz and $Q_0 = 51\,107$ for the large QTF, and $\omega_0/2\pi = 32\,766$ Hz and $Q_0 = 54\,745$ for the small QTF at a base temperature of 297.4K. The preamplifier is configured with 15 M Ω resistance and a LF357 OP-AMP. The complex gain is composed of the phase shifter and the variable gain with which one can control the damping force.

IV. RESULTS AND DISCUSSION

Figures 3(a) and 4(a) show the measured spectra S_{x+x_n} for the large and small QTF while their actual displacement spectra S_x are plotted in Figs. 3(b) and 4(b). Note that although there is no gain $|g| = 0$, the right-hand side of S_{x+x_n} is slightly

lower than the left-hand side of the floor unlike the symmetric harmonic function. This distortion is due to \bar{C}_0 which is an intrinsic property of the QTF resulting in nonmotional current. The measured values of \bar{C}_0 are 464 and 399 [29] for the large and small QTF, respectively.

As the gain increases, S_x slightly shifts to the right since there is a phase lag due to the nonideal electrical components with the increase of gain. We can fully analyze the magnitude of this residual phase difference with Eqs. (3) and (4) [30]. For large gains ($|g| > 20$), the spectra dips below the white noise floor, while the area under the actual displacement spectra curve is increased. This indicates that, when the peak of the spectrum approaches the measurement noise level, the dissipative force negatively acts to heat the resonator's vibrational mode rather than to squeeze it. We conjecture that this backaction results from the measurement noise associated with the electrical shot noise [9]. From fits of Eq. (7) to these spectra we find $\sqrt{S_{x_n}} \simeq 2.78 \times 10^{-4} \text{Å}/\sqrt{\text{Hz}}$ for the large QTF and $\sqrt{S_{x_n}} \simeq 1.97 \times 10^{-3} \text{Å}/\sqrt{\text{Hz}}$ for the small QTF.

The effective temperature T_{eff} is obtained by inputting parameters extracted from each of the spectra in Figs. 3(a) and 4(a) into Eq. (7). The minimum T_{eff} obtained in the experiment was $16.7 \pm 0.1 \text{K}$ for the large QTF and $28.7 \pm 0.1 \text{K}$ for the small QTF. These results are consistent with our analytical minimum temperature of $T_{\text{eff,min}} = 16.0 \text{K}$ for large QTF and $T_{\text{eff,min}} = 28.7 \text{K}$ for small QTF obtained from Eq. (8). Note that even though the large QTF has almost 16 times higher k and effective mass, since the level of S_{x_n} is 100 times smaller than the small QTF, the T_{eff} of the large QTF is smaller than the T_{eff} of the small QTF. The level of S_{x_n} is one of the deterministic parameters for the massive quartz-resonator cooling.

The parameters w_{eff} and Q_{eff} can be also independently measured from the electrically driven resonance curves with Q control (see Refs. [18,26] for more details). The resonance curve A_e is given by

$$A_e = \frac{I_0 \bar{w}_{\text{eff}}}{Q} \sqrt{\frac{\{[1 + \bar{C}_0(1 - \bar{w}_{\text{eff}}^2)]^2 + (\frac{\bar{C}_0 \bar{w}_{\text{eff}}}{Q_{\text{eff}}})^2\}}{(1 - \bar{w}_{\text{eff}}^2)^2 + (\frac{\bar{w}_{\text{eff}}}{Q_{\text{eff}}})^2}}, \quad (9)$$

where I_0 is the driving current. Figures 3(c) and 4(c) show the measured A_e for the large and small QTF. There is also the distortion due to the \bar{C}_0 on the right-hand side of A_e . By fitting the curves with Eq. (9), we can independently obtain w_{eff} and Q_{eff} . By inputting these parameters into Eq. (7), we also calculate $T_{\text{eff,res}}$ which can be compared to T_{eff} . $T_{\text{eff,res}}$ is $18.8 \pm 1.0 \text{K}$ for the large QTF and $31.2 \pm 0.4 \text{K}$ for the small QTF. Figure 5 shows that these two measurements of the temperatures are in reasonable agreement with each other.

Given that the resonance frequencies of the fundamental mode of the QTFs are approximately 32 kHz, to generate the nonclassical oscillator states, the $T_{\text{eff,min}}$ of QTF is required to be under the $\hbar w_0/k_B$ which is on the order of micro-Kelvin at 32 kHz. Although it is difficult to achieve this limit, it may be possible by lowering the S_{x_n} . According to Eq. (8), in order to get close to the micro-Kelvin level, $\sqrt{S_{x_n}}$ of the QTF needs to be lowered down to $\sim 10^{-8} \text{Å}/\sqrt{\text{Hz}}$ at $T_0 =$

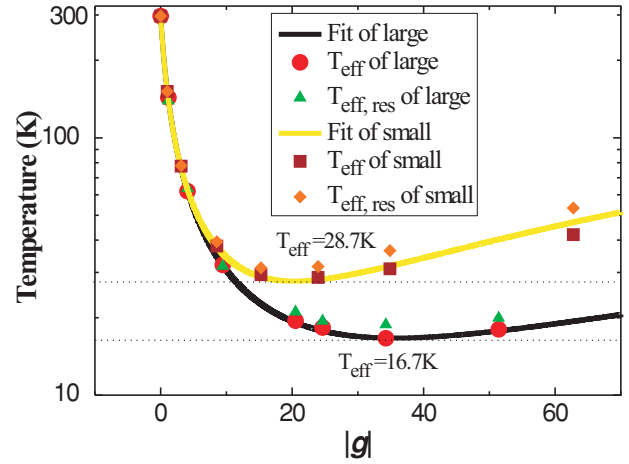


FIG. 5. (Color online) Effective temperatures of QTFs. The black (upper) solid curve is the fit of effective temperature for the large QTF from Eq. (7). The yellow (light gray) solid curve is a fit for the small QTF. The red circle is T_{eff} calculated by the extracted parameters from the measured spectra for the large QTF and the dark red square is for the small QTF. Green triangle is $T_{\text{eff,res}}$ calculated by measuring w_{eff} and Q_{eff} from the resonance curve for the large QTF and orange lozenge is for the small QTF.

4.2 K. This limit is quite achievable because the $\sqrt{S_{x_n}}$ of a QTF can be drastically lowered with the use of a low-noise device such as a single-electron transistor (SET) [31] or GaAs MESFET [32] for the preamplifier, and that can be further decreased in a cryostat [27]. In particular, SET has achieved $10^{-5} e/\sqrt{\text{Hz}}$, which indicates that a charge variation of $10^{-5} e$ can be detected in a measurement time of 1 s. This implies that the level of measurement noise for the preamplifier may be further decreased down by using the SET. It might also be a useful readout device for this massive electromechanical feedback cooling.

Furthermore, a high resonance frequency is one of the important factors needed for a massive resonator to achieve the low mean occupation number $n = k_B T/\hbar w_0$. One may obtain the quantum limited measurement with a high w_0 quartz resonator under more attainable conditions. For example, for a quartz resonator resonating at 1GHz, the quantum limited temperature is 50 mK. Thus, the resonator may be cooled down to its ground state under higher S_{x_n} or under room temperature with this active feedback cooling technique.

V. CONCLUSION

We have demonstrated a general method for active feedback cooling of massive quartz resonators. We have cooled down large and small size commercial QTFs from room temperature (297.4 K) to $16.7 \pm 0.1 \text{K}$ (large) and $28.7 \pm 0.1 \text{K}$ (small), respectively. From these results, we find that several characteristic constants k , Q , S_{x_n} , and w_0 are important parameters for massive quartz-resonator cooling. As previously noted we can obtain an extremely low S_{x_n} by using conventional cryogenic techniques and a low-noise device. Combining with a high w_0 quartz resonator may allow us to approach the quantum regime at macroscale. Moreover, since we make the feedback

cooling theory of a general equivalent circuit of a quartz resonator, our cooling mechanism can be applied to any other resonator modeled by Fig. 1(c). One may even expect the QTF as a quantum sensor for the quantum control [33] by coupling with other quantum systems such as Bose-Einstein condensation [14], dipolar molecules [15], and cold-atom system [16].

ACKNOWLEDGMENTS

We are grateful to Y. Kim and G. Moon for helpful discussions and to S. Ahn for technical support. This work was supported by the Acceleration Research Program of the Korean Ministry of Science and Technology. C. Stambaugh acknowledges support from NSF-OISE Grant 0853104.

-
- [1] K. C. Schwab and M. L. Roukes, *Phys. Today* **58**, 36 (2005); T. J. Kippenberg and K. J. Vahala, *Science* **321**, 1172 (2008).
- [2] H. Metzger, and K. Karrai, *Nature (London)* **432**, 1002 (2004).
- [3] A. Schliesser, P. Del’Haye, N. Nooshi, K. J. Vahala, and T. J. Kippenberg, *Phys. Rev. Lett.* **97**, 243905 (2006); A. Schliesser, O. Arcizet, R. Riviere, G. Anetsberger, and T. J. Kippenberg, *Nat. Phys.* **5**, 509 (2009).
- [4] J. D. Thompson, B. M. Zwickl, A. M. Jayich, F. Marquardt, S. M. Girvin, and J. G. E. Harris, *Nature (London)* **452**, 72 (2008); S. Groblacher, J. B. Hertzberg, M. R. Vanner, G. D. Cole, S. Gigan, K. C. Schwab, and M. Aspelmeyer, *Nat Phys.* **5**, 485 (2009); G. Anetsberger, O. Arcizet, Q. P. Unterreithmeier, R. Riviere, A. Schliesser, E. M. Weig, J. P. Kotthaus, and T. J. Kippenberg, *ibid.* **5**, 909 (2009); Y.-S. Park and H. Wang, *ibid.* **5**, 489 (2009).
- [5] W. Marshall, C. Simon, R. Penrose, and D. Bouwmeester, *Phys. Rev. Lett.* **91**, 130401 (2003); S. Gigan *et al.*, *Nature (London)* **444**, 67 (2006).
- [6] T. Corbitt, Y. Chen, E. Innerhofer, H. Muller-Ebhardt, D. Ottaway, H. Rehbein, D. Sigg, S. Whitcomb, C. Wipf, and N. Mavalvala, *Phys. Rev. Lett.* **98**, 150802 (2007).
- [7] O. Arcizet, P. F. Cohadon, T. Briant, M. Pinard, A. Heidmann, J. M. Mackowski, C. Michel, L. Pinard, O. Francais, and L. Rousseau, *Phys. Rev. Lett.* **97**, 133601 (2006).
- [8] D. Kleckner and D. Bouwmeester, *Nature (London)* **444**, 75 (2005).
- [9] M. Poggio, C. L. Degen, H. J. Mamin, and D. Rugar, *Phys. Rev. Lett.* **99**, 017201 (2007).
- [10] T. Corbitt, C. Wipf, T. Bodiya, D. Ottaway, D. Sigg, N. Smith, S. Whitcomb, and N. Mavalvala, *Phys. Rev. Lett.* **99**, 160801 (2007).
- [11] A. Vinante *et al.*, *Phys. Rev. Lett.* **101**, 033601 (2008).
- [12] M. D. LaHaye, O. Buu, B. Camarota, and K. C. Schwab, *Science* **304**, 74 (2004); A. Naik, O. Buu, M. D. LaHaye, A. D. Armour, A. A. Clerk, M. P. Blencowe, and K. C. Schwab, *Nature (London)* **443**, 193 (2006); M. D. LaHaye, J. Suh, P. M. Echternach, K. C. Schwab, and M. L. Roukes, *ibid.* **459**, 960 (2009); A. D. O’Connell *et al.*, *ibid.* **463**, 72 (2010).
- [13] K. R. Brown, J. Britton, R. J. Epstein, J. Chiaverini, D. Leibfried, and D. J. Wineland, *Phys. Rev. Lett.* **99**, 137205 (2007).
- [14] P. Treutlein, D. Hunger, S. Camerer, T. W. Hansch, and J. Reichel, *Phys. Rev. Lett.* **99**, 140403 (2007).
- [15] S. Singh, M. Bhattacharya, O. Dutta, and P. Meystre, *Phys. Rev. Lett.* **101**, 263603 (2008).
- [16] A. A. Geraci and J. Kitching, *Phys. Rev. A* **80**, 032317 (2009).
- [17] J. Zelenka, *Piezoelectric Resonators and Their Applications* (Elsevier, New York, 1986).
- [18] J. Jahng, *et al.* *Appl. Phys. Lett.* **91**, 023103 (2007).
- [19] F. J. Giessibl, *Rev. Mod. Phys.* **75**, 949 (2003).
- [20] J. A. Sidles, *Phys. Rev. Lett.* **68**, 1124 (1992); D. Rugar, R. Budakian, H. J. Mamin, and B. W. Chui, *Nature (London)* **430**, 329 (2004).
- [21] M. Bode, *Rep. Prog. Phys.* **66**, 523 (2003).
- [22] Y. Sugimoto, P. Pou, M. Abe, P. Jelinek, R. Perez, S. Morita, and O. Custance, *Nature (London)* **446**, 64 (2007).
- [23] Y.-J. Yu, H. Noh, G. S. Jeon, H.-R. Noh, Y. Arakawa, and W. Jhe, *Appl. Phys. Lett.* **91**, 041117 (2007).
- [24] P. D. Ashby, *Appl. Phys. Lett.* **91**, 254102 (2007).
- [25] M. Lee, B. Sung, N. Hashemi, and W. Jhe, *Faraday Discuss.* **141**, 415 (2009).
- [26] M. Lee, J. Jahng, K. Kim, and W. Jhe, *Appl. Phys. Lett.* **91**, 023117 (2007).
- [27] J. Rychen, T. Ihn, P. Studerus, A. Herrmann, K. Ensslin, H. J. Hug, P. J. A. van Schendel, and H. J. Guntherodt, *Rev. Sci. Instrum.* **71**, 4 (2000).
- [28] However, since C_0 is an intrinsic small property of the entire circuit, it may not practically control the temperature.
- [29] Typically C is on the order of 10^{-15} F, and C_0 is on the order of 10^{-13} F.
- [30] Note that even if the phase shift θ is set to $-\alpha$, a residual phase difference remains with increase of gain. This is due to the phase lags associated with the nonideal electrical components of the complex gain such as Op-Amp, capacitance, and so on. Here the residual phase lag is altered from 0 to -39.3° with the gain increase. According to the diagram of Fig. 2, the effective resonance frequency is expected to shift to the higher frequency.
- [31] M. H. Devoret, and R. J. Schoelkopf, *Nature (London)* **406**, 1039 (2000).
- [32] H. Birk, K. Oostveen, and C. Schonenberger, *Rev. Sci. Instrum.* **67**, 2977 (1996).
- [33] G. Brida, M. Genovese, and I. Ruo Berchera, *Nat. Photon.* **4**, 227 (2010).